10.24425/acs.2026.1542

Archives of Control Sciences
Volume 36(LXXII), 2026
No. 2, *pages* 391–424

Design and experimental validation of a robust dual-loop Smith predictor controller for stable and integrative systems

Nadir FERGANI and Mourad ALLAD

Time-delay systems, which are widely encountered in industrial processes, pose significant challenges to controller design due to their complex dynamics and their limited robustness margins. This paper presents an explicit design methodology for a robust Smith predictor-based control structure employing a fully isolated dual-loop configuration. The proposed controller combines integer and fractional order dynamic operators to enhance robustness against plant uncertainties while maintaining favorable dynamic performance.

The effectiveness of the proposed approach is demonstrated through simulation studies on various integrative process models, including comparative analysis with several recent control techniques. Furthermore, experimental validation on a liquid level control system representative of FOPTD industrial processes confirms the simulation findings, showing excellent reference tracking, effective disturbance rejection, and smooth control effort even under increased time delays.

The results demonstrate the superior robustness and flexibility of the proposed design compared to existing methods, highlighting the practical benefits of the isolated dual-loop Smith predictor structure for real industrial applications.

Key words: Fractional-order controller, Smith predictor, First-order-plus-time-delay (FOPTD) system, dead-time compensation, process control.

1. Introduction

Large categories of industrial processes exhibit dead time in their dynamic models, which significantly complicates both control design and system analysis.

Copyright © 2026. The Author(s). This is an open-access article distributed under the terms of the Creative Commons Attribution-NonCommercial-NoDerivatives License (CC BY-NC-ND 4.0 https://creativecommons.org/licenses/by-nc-nd/4.0/), which permits use, distribution, and reproduction in any medium, provided that the article is properly cited, the use is non-commercial, and no modifications or adaptations are made

N. Fergani (corresponding author, e-mail: nadirfergani@yahoo.fr) is with Research Center in Industrial Technologies CRTI, P.O. Box 64, Cheraga, Algiers, 16014, Algeria 00213660660105.

M. Allad (e-mail: mourad.allad@ummto.dz) is with Laboratoire Vision Artificielle et Automatique des Systèmes (LVAAS), Automatic Department, Faculty of Electrical Engineering and Computer Science, Tizi-Ouzou University, Algieria.

Received 05 Januray 2026. Revised 14 April 2026. Accepted 19 April 2026.

The time delay can be negligible, significant, or even dominant, depending on the ratio between the process dead time and its time constant [1]. Indeed, the presence of this phenomenon often degrades system performance and even leads to instability. To address this issue, particularly for processes with large dead times, various dead-time compensators have been developed, starting with the classical Smith Predictor (SP) [2]. Although this strategy is highly effective for stable systems, its applicability remains limited when the process exhibits integrating behavior or instability.

To overcome the limitations of the classical Smith Predictor (SP), the research community has extensively investigated various modifications of the Smith Predictor (SP)SP structure [3–6]. The common underlying concept among these approaches lies in the introduction of linear filters designed to minimize the mismatch between the measured and predicted plant outputs. In recent years, the Filtered Smith Predictor (FSP) has gained considerable attention, as several improved architectures have been proposed to enhance its robustness and disturbance rejection capability, especially for unstable and integrating processes.

The tuning of the Smith predictor-based controllers remains challenging due to the complex nature of the closed-loop structure, particularly in the disturbance rejection loop. Numerous studies have addressed this issue through different design methodologies. The Internal Model Control (IMC)-based tuning method was proposed in [7] for integrating processes and later extended in [8] for unstable or non-minimum phase systems. A model-adaptive Smith predictor has been developed in [9], incorporating a delayed filter, while a gain-scheduled SP approach was presented in [10]. The direct synthesis approach has been employed in [11] for unstable systems and in [12] for non-minimum phase plants. Furthermore, a feed-forward extension of the SP was introduced in [13] to deal with measurable disturbances effectively. A series cascade configuration was reported in [14], and more recently, an advanced dual-loop structure was proposed in [15], allowing for a complete isolation between the servo and regulatory loops. A resilient dual-loop control framework has been experimentally validated to maintain stable operation of process systems under cyberattacks, ensuring smooth controller switching and rapid recovery without process shutdown [16].

Recent years have a remarkable shift in control research toward incorporating fractional calculus into Smith Predictor (SP) structures, aiming to improve robustness and adaptability for time-delay systems. The first notable application was reported by Feliu-Batlle et al. [17], where a fractional-order controller was integrated with the SP for controlling an irrigation canal pool, ensuring superior performance compared with conventional robust control schemes. Following this, Boudjehem et al. [18] proposed a fractional-order model-based prediction scheme, in which an optimized fractional strategy improved closed-loop accuracy

and dynamic response. The fractional PI controller was then embedded into the classical SP in [19], showing consistent superiority in both servo and regulatory operations. Bettayeb et al. [20] introduced a model-based analytical synthesis method combining fractional-order controllers with both conventional and modified SP structures, resulting in highly robust control laws for long time-delay processes. Similarly, Safaei and Tavakoli [21] developed a simple analytical design procedure for fractional-order controllers applied to integer-order systems with delay, exploiting a time-domain design concept. To enhance sensitivity and robustness, Nagarsheth and Sharma [22] proposed thea combination of a fractional filter and athe Smith pPredictor, demonstrating significant improvement in maximum sensitivity performance. Advanced Smith Predictor-based adaptive fractional-order control strategies have been developed to improve robustness, tracking performance, and delay compensation in high-precision systems [23].

Further developments include Laifa et al. [24], who extended the direct synthesis concept to design fractional-order PID controllers embedded in SP structures for both SISO and MIMO fractional systems, achieving efficient regulation of non-integer order models. In [25], a two-degree-of-freedom (2-DOF) fractional-order IMC-based SPmith predictor was developed for a coupled two-tank process, providing analytically tuned servo and regulatory controllers with improved disturbance rejection. Deniz [26] introduced an effective SP-based FOPID design methodology relying on Bode's Ideal Transfer Function (BITF) and continued fraction expansion (CFE), addressing optimality and actuator saturation constraints. Saikumar et al. [27] extended the fractional IMC-PID combined with the SP for nonlinear chemical processes, demonstrating robust performance under strong process-model mismatch. A direct synthesis fractional-order controller for integrating plants was also proposed in [28], where the resulting structure showed similarity to the filtered SP approach. The literature reports extensive developments of modified Smith Predictor (MSP) schemes to overcome the limitations of conventional SP in time-delay systems, particularly for integrating and unstable processes under uncertainty and noise [29].

More recently, the design of fractional-order IMC-based Smith pPredictors for unstable and delay-dominant processes has gained attention. Ranjan and Mehta [30] developed a fractional-order tilt-integral-derivative (FOTID) controller under the IMC scheme for unstable systems, while Muresan and Birs [31] analyzed fractional PI control for unstable first-order delayed processes. Nguyen et al. [32] proposed analytical frequency-domain tuning rules for fractional cascade structures, and Singha et al. [33] presented a 2-DOF fractional-order control structure integrated with the SP, offering explicit tuning formulas based on phase margin and maximum sensitivity criteria. A robust cascade configuration was later formulated by Singha et al. [34], capable of maintaining stability under 70%

delay variation and 60% gain uncertainty. Meena et al. [35] further introduced dual-parametric fractional controllers for stable, unstable, and integrating delayed plants with experimental validation. Lastly, Aryan et al. [36] proposed a robust shifted-IMC-based modified decoupled Smith Predictor (RDSP), which demonstrated improved performance in delay-dominant chemical processes. More recently, a dual parametric fractional-order tuning is presented in [37] based on maximum sensitivity function. A similar technique has been proposed in [38] for delay-dominant processes.

Despite significant advancements, intensive research efforts are still ongoing in this field. Explicit formulations of robustness metrics, such as maximum sensitivity (M_s), remain challenging within fractional order SP configurations. In addition, the relationship between robustness, quantified by M_s, and the structural variations of SP schemes has not been investigated in the existing literature.

In this work, the isolated loop SP structure proposed in [15] is combined to fractional order controller to enhances the robustness-performance trade-off of the closed loop system. The proposed controller is analytically designed, based on (M_s) robustness criterion, using analytical solutions of cubic and quartic polynomial equations. The main contributions are:

- An analytically tuned dual-loop control scheme is proposed for both stable (FOPDT) and integrating processes.
- The robustness of the tow isolated controller will be studied separately.

The reminder of the paper is organized as following: Section 2 presents the proposed control strategy. Section 3 details the controller design mythologies for case of the (FOPDT) system. Sections 4 and 5 investigate the control of first- and second-order integrating plants, respectively. Section 6 provides simulation results obtained for stable and integrative system. Finally, Section 7 concludes the paper.

2. Smith predictor based control strategy

Figure 1 illustrates the conventional filtered Smith Predictor (FSP) where the linear filter $F(s) = 1$ for conventional smith predictor configuration. The inclusion of $F(s)$ allows additional flexibility in shaping the disturbance rejection loop as in [6] where an explicit tuning has been formulated.

$P(s) = G_p(s)e^{-\theta s}$ denotes the plant transfer function where $G_p(s)$ is the delay free part of the process. $G_m(s)$ is the nominal delay-free model of the plant is, while $G_c(s)$ is the controller transfer function. The nominal plant including delay is expressed as $P^*(s) = G_m(s)e^{-\theta s}$.

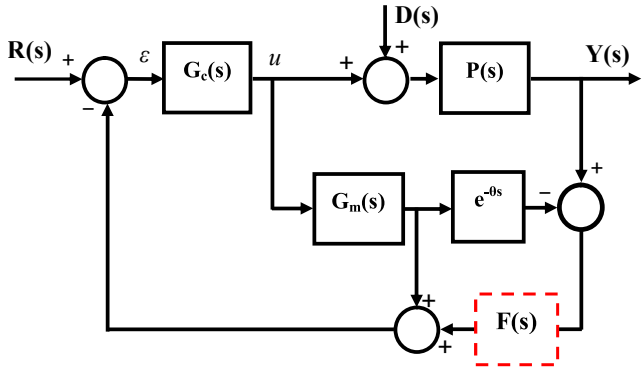


Figure 1: Conventional Filtered Smith predictor structure

The closed loop transfer functions for nominal case are given by:

$$\begin{aligned} \frac{Y(s)}{R(s)} &= \frac{G_c(s)G_m(s)e^{-\theta s}}{1+G_{c1}(s)G_m(s)}, \\ \frac{Y(s)}{D(s)} &= P^*(s)\left(1-\frac{F(s)G_c(s)G_m(s)e^{-\theta s}}{1+G_c(s)G_m(s)}\right). \end{aligned} \tag{1}$$

Recently, a completely isolated structure have been proposed in [15] (Fig. 2).

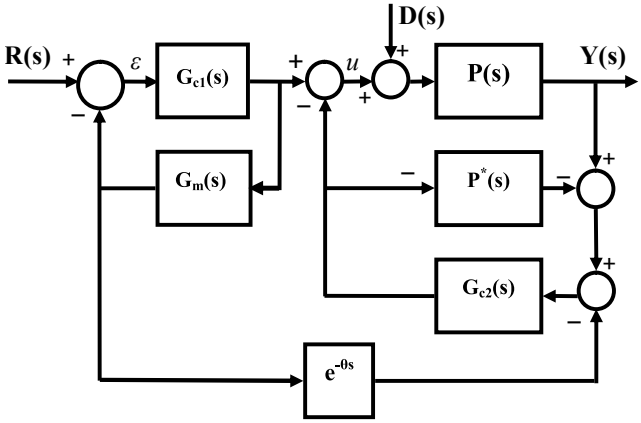


Figure 2: Advanced decoupled dual-loop smith predictor structure

The closed loop transfer functions are given by:

$$\begin{aligned} \frac{Y(s)}{R(s)} &= \frac{G_c(s)G_p(s)e^{-\theta s}}{1+G_{c1}(s)G_p(s)}, \\ \frac{Y(s)}{D(s)} &= G_p(s)e^{-\theta s}\left(1-G_{c2}(s)G_p(s)e^{-\theta s}\right). \end{aligned} \tag{2}$$

It is evident that these two loops can be designed independently through the controllers $G_{c1}(s)$ and $G_{c2}(s)$. Accordingly, two distinct sensitivity functions are associated with the tracking and disturbance rejection loops. In this work, a fractional-order controller is employed for the tracking loop to enhance flexibility and robustness, while an integer-order robust controller is adopted for the disturbance loop, denoted as $G_{c2}(s)$.

3. Controller design

In this section, the controllers are designed for a First-Order Plus Dead Time (FOPDT) system, which is expressed as:

$$P(s) = \frac{k}{1+Ts} e^{-\theta s}, \tag{3}$$

where k is the steady-state gain, T represents the process time constant, and θ denotes the time delay.

3.1. Tracking controller design $G_{c1}(s)$

Since the first introduction of fractional calculus into control theory by the CRONE research team [39], its principal advantage has been the ability to employ Bode's Ideal Transfer Function (BITF) as a reference model for controller design. This ideal transfer function is defined as:

$$\begin{aligned} L(s) &= \frac{1}{(s/\omega_c)^m}, \\ G(s) &= \frac{1}{1+(s/\omega_c)^m} n, \end{aligned} \tag{4}$$

where $L(s)$ and $G(s)$ denote the open-loop and closed-loop transfer functions, respectively.

This reference model is used to design the controller for delay free part of the plant as demonstrated in [26]. The controller parameters can be directly computed using the explicit formulas provoided in [40] where for FOPDT systems the delay free controller is expressed as:

$$\begin{aligned} G_{c1}(s) &= k_c + \frac{T_i}{s^\lambda} + T_d s^\mu, \\ k_c = 0; \quad T_i &= \frac{\omega_c^m}{k}; \quad T_d = TT_i; \quad \lambda = m; \quad \mu = 1-m. \end{aligned} \tag{5}$$

All other general stable plants are summarized in [40].

For robustness assessment, the most widely adopted metric is the maximum sensitivity function, which is defined as:

$$M_s = \|S(s)\|_\infty = \left\| \frac{1}{1 + G_{c1}(s)P(s)} \right\|_\infty = \left\| \frac{(s/\omega_c)^m}{(s/\omega_c)^m + e^{-\theta s}} \right\|_\infty . \tag{6}$$

This value reflects the system's sensitivity to model uncertainties and external disturbances. A lower M_s indicates higher robustness, as the system becomes less sensitive to variations. Typically, acceptable values for robust control design fall within the range $1.2 < M_s < 2$, ensuring a good compromise between performance and robustness.

Controller (5) contains two parameters to be tuned m and ω_c. The first one m, directly influences the system overshoot. To simplify the analytical design and reduce computational complexity, this parameter is fixed to a recommended value. For instance, $m = 1.1$ typically corresponds to a moderate overshoot of about 3%.

By introducing the new variable $\tau_c = 1/\omega_c^m$, the sensitivity function can be expressed as:

$$S(s) = \frac{\tau_c s^m}{\tau_c s^m + e^{-\theta s}} . \tag{7}$$

The magnitude of the sensitivity function is then given by:

$$|S(j\omega)| = \frac{\tau_c \omega^m}{\sqrt{\left(\omega^m \cos\left(\frac{m\pi}{2}\right)\tau_c + \cos(\theta\omega)\right)^2 + \left(\omega^m \sin\left(\frac{m\pi}{2}\right)\tau_c - \sin(\theta\omega)\right)^2}} \tag{8}$$

At the frequency $\omega = \omega_p$ the magnitude reaches its maximum value, corresponding to the maximum sensitivity M_s:

$$M_s = \frac{\tau_c \omega_p^m}{\sqrt{\left(\omega_p^m \cos\left(\frac{m\pi}{2}\right)\tau_c + \cos(\theta\omega_p)\right)^2 + \left(\omega_p^m \sin\left(\frac{m\pi}{2}\right)\tau_c - \sin(\theta\omega_p)\right)^2}} \tag{9}$$

by algebraic manipulation of (9), the following second order equation in τ_c is obtained:

$$a\tau_c^2 + b\tau_c + c = 0 \tag{10}$$

where the coefficients are defined as:

$$\begin{aligned} a &= \left(M_s^2 - 1\right)\omega_p^{2m}, \\ b &= 2M_s^2 \omega_p^{2m} \cos\left(\frac{m\pi}{2} + \theta\omega_p\right), \\ c &= M_s^2 . \end{aligned} \tag{11}$$

The values of τ_c are given by:

$$\tau_{c1,2} = \frac{-b \pm \sqrt{\Delta}}{2a}, \tag{12}$$

with the discriminant given by: $\Delta = M_s^2 \omega_p^{2m} \left(2M_s^2 \cos\left(m\pi + 2\theta\omega_p\right) - 2M_s^2 + 4\right)$.

In the other hand, the magnitude of eq. (8) reaches its maximum when its derivative with respect to ω is equal to zero, this condition can be expressed as:

$$\left.\frac{d\,|S(j\omega)|}{d\omega}\right|_{\omega=\omega_p} = 0 \tag{13}$$

which lead us to derivate the following equation:

$$A\tau_c^3 + B\tau_c^2 = 0, \tag{14}$$

where

$$\begin{aligned} A &= 2\omega_p^{3m}\left(m\cos\left(\frac{m\pi}{2} + \theta\omega_p\right) + \theta\omega_p \sin\left(\frac{m\pi}{2} + \theta\omega_p\right)\right), \\ B &= 2m\omega_p^{2m}. \end{aligned} \tag{15}$$

Since τ_c is strictly positive value, only one solution is admissible, given by:

$$\tau_{c3} = \frac{-B}{A}. \tag{16}$$

From equations (12) and (16) the tuning parameter τ_c is expressed as function of the peak frequency ω_p which is generally located generally within the dynamic performance frequency band. In this study, the frequency range of $[1/T$ to $20/T]$ is considered for ω_p.

Tuning procedure for tracking controller (FOPDT)

Required inputs: process parameters k, T, θ from the identified model and the desired M_s.

- **Step 1:** Select the fractional order m according to desired overshoot specification.
- **Step 2:** Plot the curve of τ_{c2} from eq. (12) using parameters defined in eq. (11).
- **Step 3:** Plot the curve of τ_{c3} from eq. (16) using parameters defined in eq. (15). Then determine τ_c from the intersection point of the two curves (12) and (16). Compute $\omega_c = (\tau_c)^{1/m}$.
- **Step 4:** Tune the fractional order controller using equation (5).

3.2. Disturbance controller design $G_{c2}(s)$

From equation (2), the sensitivity function associated with the second loop is expressed as:

$$S(s) = \left(1 - G_{c2}(s)G_p(s)e^{-\theta s}\right). \tag{17}$$

According to tuning approach presented in [6], the controller $G_{c2}(s)$ can be designed in the same way to the filter that used to compensates the slow or undesirable dynamics of the plants. In this work, the following structure is considered:

$$G_{c2}(s) = \frac{1}{k}\frac{(1+Ts)\,(1+\beta s)}{(1+T_o s)^2}. \tag{18}$$

As the closed loop disturbance transfer function is given by $S(s)G_p(s)e^{-\theta s}$. Applying the first order Padé approximation for the exponential term, the sensitivity transfer function can be written as:

$$S(s) = \left(\frac{\left(1+\frac{\theta}{2}s\right)(1+T_o s)^2 - (1+\beta s)\left(1-\frac{\theta}{2}s\right)}{(1+T_o s)^2\left(1+\frac{\theta}{2}s\right)}\right). \tag{19}$$

The parameter β is selected such that $s = -1/T$ becomes a zero of $S(s)$, leading to:

$$\beta = \frac{2T^2 - 2TT_o + T_o^2}{T} - \frac{4(T-T_o)^2}{2T+\theta}. \tag{20}$$

Chosen β according to (20), the sensitivity function becomes:

$$S(s) = \frac{s\left(s+\frac{1}{T}\right)(\alpha s+\gamma)}{(1+T_o s)^2\left(1+\frac{\theta}{2}s\right)}, \tag{21}$$

where the coefficients α and γ are defined as:

$$\begin{aligned} \alpha &= \frac{T_o^2\theta}{2}, \\ \gamma &= T\,(2T_o - \beta + \theta). \end{aligned} \tag{22}$$

From equation (21), the magnitude of the sensitivity function is given by:

$$|S(j\omega)| = \frac{\omega\sqrt{\omega^2+T^{-2}}\sqrt{\alpha^2\omega^2+\gamma^2}}{\left(1+T_o^2\omega^2\right)\sqrt{1+(\theta\omega/2)^2}} \tag{23}$$

at the frequency $\omega = \omega_p$ the magnitude reach its maximum value:

$$M_s = \frac{\omega_p \sqrt{\omega_p^2 + T^{-2}} \sqrt{\alpha^2 \omega_p^2 + \gamma^2}}{\left(1 + T_o^2 \omega_p^2\right) \sqrt{1 + \left(\theta \omega_p / 2\right)^2}}. \tag{24}$$

By algebraic manipulations of eq. (24), the following high-order polynomial equation is obtained:

$$a_\omega \omega_p^6 + b_\omega \omega_p^4 + c_\omega \omega_p^2 + d_\omega = 0, \tag{25}$$

where the coefficients are expressed as:

$$\begin{aligned} a_\omega &= 0.25 M_s^2 T_o^4 \theta^2 - \alpha^2, \\ b_\omega &= M_s^2 T_o^4 \theta^2 - \frac{\alpha^2}{T^2} - \gamma^2 + 0.5 M_s^2 T_o^2 \theta^2, \\ c_\omega &= 2 M_s^2 T_o^2 - \frac{\gamma^2}{T^2} + 0.25 M_s^2 \theta^2, \\ d_\omega &= M_s^2 . \end{aligned} \tag{26}$$

By introducing the substitution $x = \omega^2$, eq. (25) can be transformed into the following cubic polynomial form:

$$a_\omega x^3 + b_\omega x^2 + c_\omega x + d_\omega = 0. \tag{27}$$

This equation always admits at least one real root, which can be explicitly determined using the Cardano formula as:

$$x_0 = \sqrt[3]{\frac{-q}{2} + \sqrt{\frac{q^2}{4} + \frac{p^3}{27}}} + \sqrt[3]{\frac{-q}{2} - \sqrt{\frac{q^2}{4} + \frac{p^3}{27}}} - \frac{b_\omega}{3a_\omega}, \tag{28}$$

where

$$\begin{aligned} p &= \frac{-b_\omega^2}{3a_\omega^2} + \frac{c_\omega}{a_\omega}, \\ q &= \frac{2b_\omega^3}{27a_\omega^2} - \frac{c_\omega b_\omega}{3a_\omega^2} + \frac{d_\omega}{a_\omega}. \end{aligned} \tag{29}$$

Then the corresponding peak frequency is obtained as:

$$\omega_{p1} = \sqrt{x_0} = f(T_o) \tag{30}$$

On the other hand, the magnitude given in equation (23) reaches its maximum value when its derivative with respect to ω becomes zero. By differentiating equation (23), the following polynomial equation is obtained:

$$f_1\omega_p^6 + f_2\omega_p^4 + f_3\omega_p^2 + f_4 = 0, \tag{31}$$

where the coefficients are expressed as:

$$\begin{aligned}
f_1 &= 0.5T^2T_o^4\theta^4 - 0.25T^2T_o^6\theta^4 + T^2T_o^6\theta^2 \\
&\quad - T^4T_o^2\theta^2\left(2T_o + \theta - \frac{2TT_o + T\theta - T_o\theta - T_o^2 + \dfrac{T_o^4\theta}{2T}}{\left(T + \dfrac{\theta}{2}\right)}\right)^2, \\
f_2 &= 0.25T_o^4\theta^4 + 3T^2T_o^4\theta^2 \\
&\quad + \frac{\left(T^2\theta^2 - 2T_o^2\theta^2\right)\left(-T_o^2\theta + 2TT_o^2 + 4TT_o\theta + T\theta^2\right)^2}{(2T+\theta)^2}, \\
f_3 &= 2T_o^4\theta^2 + \frac{\left(8T^2 - 4T_o^2\right)\left(-T_o^2\theta + 2TT_o^2 + 4TT_o\theta + T\theta^2\right)^2}{(2T+\theta)^2}, \\
f_4 &= \frac{4\left(-T_o^2\theta + 2TT_o^2 + 4TT_o\theta + T\theta^2\right)^2}{(2T+\theta)^2}.
\end{aligned} \tag{32}$$

Applying the same transformation as before, equation (31) can be reduced to cubic polynomial in $y = \omega^2$, which can be solved using Cardano formula. The resulting expression for the peak frequency is:

$$\omega_{p2} = \sqrt{y_0} = g(T_o), \tag{33}$$

where

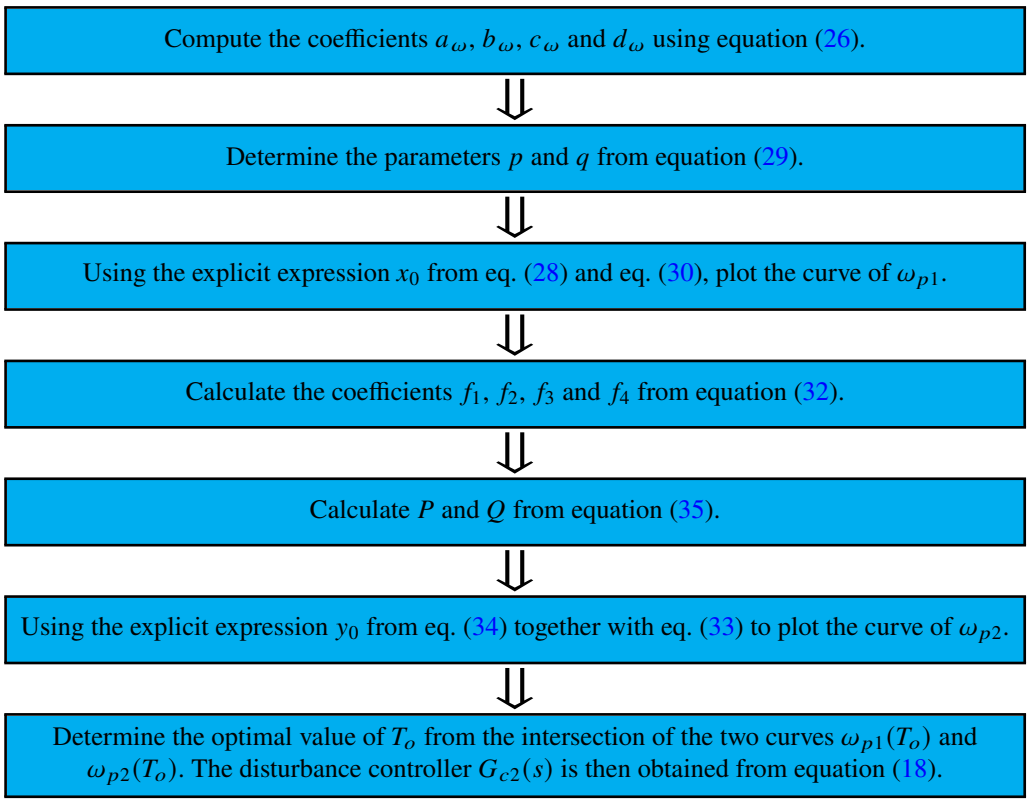
$$y_0 = \sqrt[3]{\frac{-Q}{2} + \sqrt{\frac{Q^2}{4} + \frac{P^3}{27}}} + \sqrt[3]{\frac{-Q}{2} - \sqrt{\frac{Q^2}{4} + \frac{P^3}{27}}} - \frac{f_2}{3f_1} \tag{34}$$

and

$$\begin{aligned}
P &= \frac{-f_2^2}{3f_1^2} + \frac{f_3}{f_1}, \\
Q &= \frac{2f_2^3}{27f_1^2} - \frac{f_3f_2}{3f_1^2} + \frac{f_4}{f_1}.
\end{aligned} \tag{35}$$

Proposed tuning procedure for disturbance controller (FOPDT)

Required inputs: Process parameters k, T, θ from the model and the desired M_s.



4. First order integrative plant

Considering the pure integrator delay system expressed as:

$$P(s) = \frac{k}{s} e^{-\theta s}. \tag{36}$$

The same design approach described in Section 3 can be applied to this type of system, with appropriate modifications due to the integrative nature of the process. For the tracking controller, the same procedure is maintained except the eq. (5) of the controller parameters must be changed according to [40]:

$$\begin{gathered} G_{c1}(s) = k_c + \frac{T_i}{s^\lambda} + T_d s^\mu, \\ k_c = 0; \quad T_i = \frac{\omega_c^m}{k}; \quad T_d = 0; \quad \lambda = m; \quad \mu = 1 - m. \end{gathered} \tag{37}$$

Regarding the disturbance controller, the tuning procedure follows the same principle as in Section 3, but with the necessary adjustments for the integrative model. The proposed tuning method can be summarized as follows.

Disturbance controller design $G_{c2}(s)$

Required inputs: Process parameters k and θ and the desired M_s.

Step 1: Compute the intermediate parameters α, β and γ as:

$$\begin{aligned} \alpha &= T_o^2\theta/2, \\ \gamma &= T_o^2 + 2T_o\theta + 0.5\theta^2, \\ \beta &= 2T_o + \theta. \end{aligned} \tag{38}$$

Step 2: Calculates a_ω, b_ω, c_ω and d_ω according to:

$$\begin{aligned} a_\omega &= 0.25M_s^2T_o^4\theta^2 - \alpha^2, \\ b_\omega &= M_s^2T_o^4 - \gamma^2 + 0.5M_s^2T_o^2\theta^2, \\ c_\omega &= 2M_s^2T_o^2 + 0.25M_s^2\theta^2, \\ d_\omega &= M_s^2\,. \end{aligned} \tag{39}$$

Step 3: Compute the cubic polynomial parameters p and q as:

$$\begin{aligned} p &= \frac{-b_\omega^2}{3a_\omega^2} + \frac{c_\omega}{a_\omega}\,, \\ q &= \frac{2b_\omega^3}{27a_\omega^2} - \frac{c_\omega b_\omega}{3a_\omega^2} + \frac{d_\omega}{a_\omega}\,. \end{aligned} \tag{40}$$

Step 4: Determine the first real solution of the cubic equation:

$$x_0 = \sqrt[3]{\frac{-q}{2} + \sqrt{\frac{q^2}{4} + \frac{p^3}{27}}} + \sqrt[3]{\frac{-q}{2} - \sqrt{\frac{q^2}{4} + \frac{p^3}{27}}} - \frac{b_\omega}{3a_\omega}\,. \tag{41}$$

Then plot

$$\omega_{p1} = \sqrt{x_0} = f(T_o). \tag{42}$$

Step 5: Compute the coefficients a, b and c

$$\begin{aligned} a &= 4\alpha^2T_o^2 + 2\alpha^2\theta^2 - \gamma^2T_o^2\theta^2, \\ b &= 124\alpha^2 + \gamma^2\theta^2, \\ c &= 8\gamma^2. \end{aligned} \tag{43}$$

Step 6: Solve the corresponding quadratic equation:

$$y_0 = \frac{-b - \sqrt{b^2 - 4ac}}{2a}. \tag{44}$$

Then plot

$$\omega_{p2} = \sqrt{y_0} = g(T_o). \tag{45}$$

Step 7: determine T_o from intersection point of the two curves (42) and (45) then the controller is obtained using the following structure:

$$G_{c2}(s) = \frac{1}{k}\frac{s(1+\beta s)}{(1+T_o s)^2}. \tag{46}$$

The associated sensitivity function is expressed as:

$$|S(j\omega)| = \frac{\omega^2\sqrt{\alpha^2\omega^2 + \gamma^2}}{\left(1 + T_o^2\omega^2\right)\sqrt{1 + (\theta\omega/2)^2}}. \tag{47}$$

5. Second-order integrating plus time delay system (SOIPTD)

Consider the second order integrative process with delay modeled as:

$$P(s) = \frac{k}{s(1+Ts)}e^{-\theta s} \tag{48}$$

For tracking controller, the same procedure is maintained except the eq. (5) of the controller parameters must be changed according to [40]:

$$\begin{gathered} G_{c1}(s) = k_c + \frac{T_i}{s^\lambda} + T_d s^\mu, \\ k_c = 0; \quad T_i = \frac{\omega_c^m}{k}; \quad T_d = T\frac{\omega_c^m}{k}; \quad \lambda = m - 1; \quad \mu = 2 - m. \end{gathered} \tag{49}$$

The design of the disturbance controller $G_{c2}(s)$ follows a similar analytical procedure to that used for lower-order systems, with additional terms introduced by the second-order dynamics.

Disturbance controller design $G_{c2}(s)$

Required inputs: k, T and θ from the model and the desired M_s.

Step 1: Compute the intermediate parameters α, β, γ and δ as:

$$\begin{aligned}
\alpha &= \frac{T_o^3\theta}{2}\,,\\
\beta &= 3T_o + \theta,\\
\gamma &= \frac{T\theta^3 + 6TT_o\theta^2 + \left(12TT_o^2 - 2T_o^2\right)\theta + 4TT_o^3}{4T + 2\theta}\,,\\
\delta &= 3T_o\theta - \frac{(2T_o + \theta)^3}{2(2T + \theta)} + 3T_o^2 + \frac{T_o^3}{T} + \frac{\theta^2}{2}\,.
\end{aligned} \tag{50}$$

Step 2: Calculates a_ω, b_ω, c_ω, d_ω and e_ω of the forth order polynomial as follows:

$$\begin{aligned}
a_\omega &= 0.25M_s^2T_o^6\theta^2 - \alpha^2\,,\\
b_\omega &= M_s^2T_o^6 - \gamma^2 - \frac{\alpha^2}{T^2} + 0.75M_s^2T_o^4\theta^2\,,\\
c_\omega &= 3M_s^2T_o^4 - \frac{\gamma^2}{T^2} + 0.75M_s^2T_o^2\theta^2\,,\\
d_\omega &= 3M_s^2T_o^2 + 0.25M_s^2\theta^2\,,\\
e_\omega &= M_s^2\,.
\end{aligned} \tag{51}$$

Step 3: Normalize the coefficients a_n, b_n, c_n and d_n as follows:

$$\begin{aligned}
a_n &= \frac{b_\omega}{a_\omega}\,,\\
b_n &= \frac{c_\omega}{a_\omega}\,,\\
c_n &= \frac{d_\omega}{a_\omega}\,,\\
d_n &= \frac{e_\omega}{a_\omega}\,.
\end{aligned} \tag{52}$$

Step 4: Compute the auxiliary parameters p_n, q_n and r_n

$$\begin{aligned}
p_n &= b_n - \frac{3a_n^2}{8}\,,\\
q_n &= -0.5a_nb_n + \frac{a_n^3}{8} + c_n\,,\\
r_n &= -0.25a_nc_n + \frac{a_n^2b_n}{16} - \frac{3a_n^2}{256} + d_n\,.
\end{aligned} \tag{53}$$

Step 5: Calculates a, b, c and d as follows:

$$\begin{aligned} a &= 1, \\ b &= 2p_n\,, \\ c &= p_n^2 - 4r_n\,, \\ d &= -q_n^2\,. \end{aligned} \tag{54}$$

Step 6: Compute p and q

$$\begin{aligned} p &= \frac{-b^2}{3a^2} + \frac{c}{a}\,, \\ q &= \frac{2b^3}{27a^2} - \frac{cb}{3a^2} + \frac{d}{a}\,. \end{aligned} \tag{55}$$

Step 7: Determine the first real solution of the cubic equation

$$k_0 = \left(\sqrt[3]{\frac{-q}{2} + \sqrt{\frac{q^2}{4} + \frac{p^3}{27}}} + \sqrt[3]{\frac{-q}{2} - \sqrt{\frac{q^2}{4} + \frac{p^3}{27}}} - \frac{2p_n}{3} \right)^{1/2}. \tag{56}$$

Step 8: Calculates the first peak frequency

$$\omega_{p1} = \frac{k_0 + \sqrt{k_0^2 - 2(p_n + k_0^2 + q_n/k_0)}}{2}\,. \tag{57}$$

Step 9: Calculate the second set of coefficients

$$\begin{aligned} a &= 4\alpha^2 T^2 T_o^2 + 3\alpha^2 T^2 \theta^2 - \alpha^2 T_o^2 \theta^2 - \gamma^2 T^2 T_o^2 \theta^2, \\ b &= 16\alpha^2 T^2 + 2\alpha^2 \theta^2 + 2\gamma^2 T^2 \theta^2 - 2\gamma^2 T_o^2 \theta^2, \\ c &= 12\alpha^2 + 12\gamma^2 T^2 - 4\gamma^2 T_o^2 - \gamma^2 \theta^2, \\ d &= 8\gamma^2. \end{aligned} \tag{58}$$

Step 10: Compute p and q

$$\begin{aligned} p &= \frac{-b^2}{3a^2} + \frac{c}{a}\,, \\ q &= \frac{2b^3}{27a^2} - \frac{cb}{3a^2} + \frac{d}{a}\,. \end{aligned} \tag{59}$$

Step 11: Determine the second solution

$$\omega_{p2} = \left(\sqrt[3]{\frac{-q}{2} + \sqrt{\frac{q^2}{4} + \frac{p^3}{27}}} + \sqrt[3]{\frac{-q}{2} - \sqrt{\frac{q^2}{4} + \frac{p^3}{27}}} - \frac{b}{3a} \right)^{1/2}. \tag{60}$$

Step 12: Extract T_o from intersection of the two curves (57) and (60) then the controller is obtained using the following structure:

$$G_{c2}(s) = \frac{s}{k} \frac{(1+Ts)\,(1+\beta s+\delta s^2)}{(1+T_o s)^3}. \tag{61}$$

The associated sensitivity function is expressed as:

$$|S(j\omega)| = \frac{\omega^2 \sqrt{\alpha^2\omega^2+\gamma^2}}{\left(1+T_o^2\omega^2\right)\sqrt{1+(\theta\omega/2)^2}}. \tag{62}$$

6. Results and discussion

This section presents simulation studies carried out using the MATLAB/Simulink environment, followed by experimental validation performed on a liquid level control plant.

6.1. Example 1 (second order integrative)

Consider the delay dominated process given in [41]:

$$P(s) = \frac{1}{s(1+3.4945s)} e^{-6.567s}. \tag{63}$$

Using the analytical procedure developed in Section 4, the following controller was obtained:

$$\begin{aligned} G_{c1}(s) &= \frac{(1+3.4945s)0.5^{1.1}}{s^{0.1}}, \\ G_{c2}(s) &= \frac{s\,(1+3.4945s)\left(1+24.324s+72.6617s^2\right)}{(1+5.9190s)^3} \quad (M_s = 2), \\ G_{c2}(s) &= \frac{s\,(1+3.4945s)\,(1+42.933s+132.097s^2)}{(1+12.122s)^3} \quad (M_s = 1.6). \end{aligned} \tag{64}$$

In [41], following tracking, disturbance and filter have been proposed to control the system:

$$\begin{aligned} G_{c1}(s) &= 0.6(1 + 3.4945s), \\ G_{c2}(s) &= 0.1\,(1 + 269s)\,, \\ F(s) &= \frac{1}{1 + 0.164s}\,. \end{aligned} \tag{65}$$

Time-domain simulations were performed to assess both reference tracking and disturbance rejection capabilities. The step response to a set-point change at $t = 0$ and the load disturbance rejection for $d = -0.5$ applied at $t = 300$ s are illustrated in Figure 3. To evaluate robustness, the plant parameters were varied by increasing both the process gain and time delay by 30% from their nominal values. The corresponding responses of the perturbed systems are shown in Figure 4.

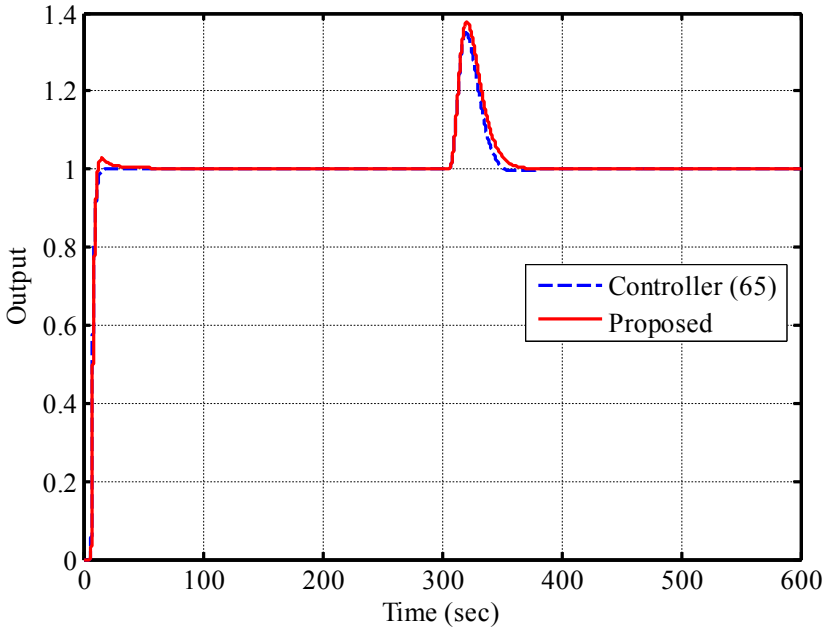


Figure 3: Time responses of Example 1 for nominal cases

It can be clearly observed that the proposed controller exhibits superior robustness compared to the controller reported in [41]. This enhanced performance is attributed to the flexibility of the proposed tuning approach, in which the selected M_s value directly determines the system sensitivity and consequently governs the robustness–performance trade-off.

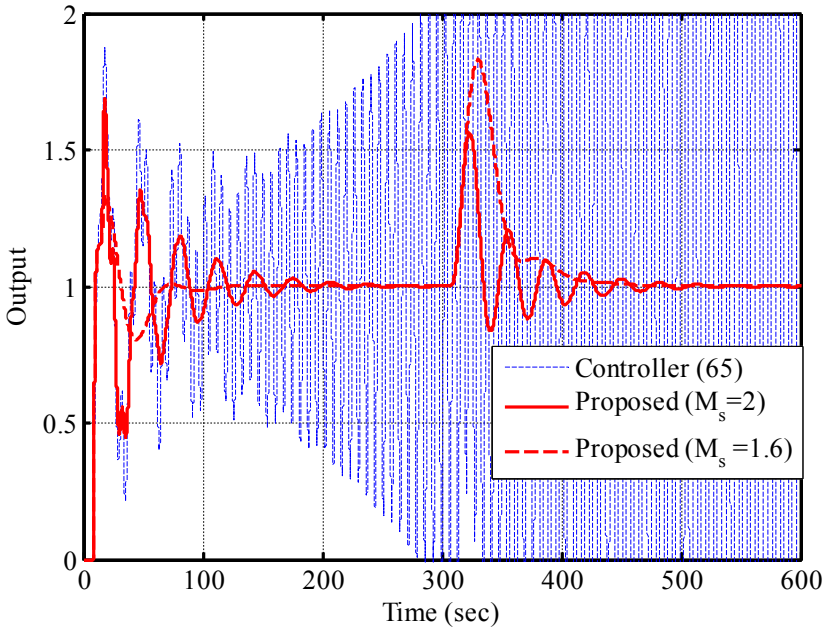


Figure 4: Time responses of Example 1 for perturbed plant (+30%)

6.2. Example 2: consider the delayed integrator system given in [42]

$$P(s) = \frac{1}{s} e^{-4s}. \tag{66}$$

For specified maximum sensitivity $M_s = 2$, The proposed controller is designed as follows:

$$\begin{aligned} G_{c1}(s) &= \frac{1}{s^{0.1}}, \\ G_{c2}(s) &= \frac{s\,(1 + 3.4945s)}{(1 + 5.9190s)^2}. \end{aligned} \tag{67}$$

For a fair comparison, the proposed controller is evaluated against the controller presented in [42], which was also designed for. This controller employs a combined PI–PD structure with a set-point (SP) configuration, and is expressed as:

$$\begin{aligned} G_{c1}(s) &= 0.039 \left(1 + \frac{1}{1.361s}\right), \\ G_{c2}(s) &= 0.195\,(1 + 1.933s). \end{aligned} \tag{68}$$

The simulation scenario includes a step change in the set-point at $t = 0$ sec and a load disturbance of $d = -0.1$ applied at $t = 200$ sec. The corresponding

time responses of the proposed controller and the controller in (68) are presented in Figures 5 and 6, representing the nominal and perturbed cases (with +30% variations in plant gain and time delay), respectively.

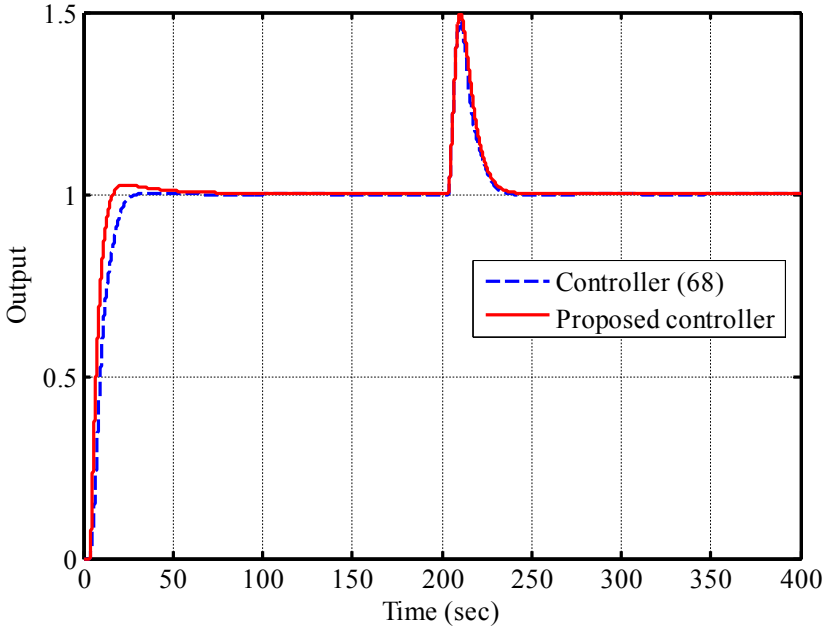


Figure 5: Time responses of Example 2 for nominal cases

From Figure 5, it can be observed that the proposed isolated-loop configuration achieves improved performance, particularly in tracking accuracy, as summarized in Table 1. Moreover, Figure 6 shows that the proposed controller provides superior disturbance rejection performance compared with the controller of [42] despite both being designed with the same M_s value.

These results can be attributed to two key factors. First, the use of a fractional-order controller in the tracking loop inherently enhances robustness against parameter variations. Second, the isolated control structure allows the disturbance rejection loop to operate more independently, improving overall robustness and disturbance attenuation.

Table 1 summarizes the performance indices in terms of the Integral of Absolute Error (IAE), Integral of Squared Error (ISE), and Total Variation (TV) of the control signal, for both controllers under three operating conditions: nominal, and perturbed cases with +15% and +30% variations in process gain and delay. The results indicate that the proposed controller achieves better tracking performance under nominal conditions and maintains superior robustness under significant parameter perturbations.

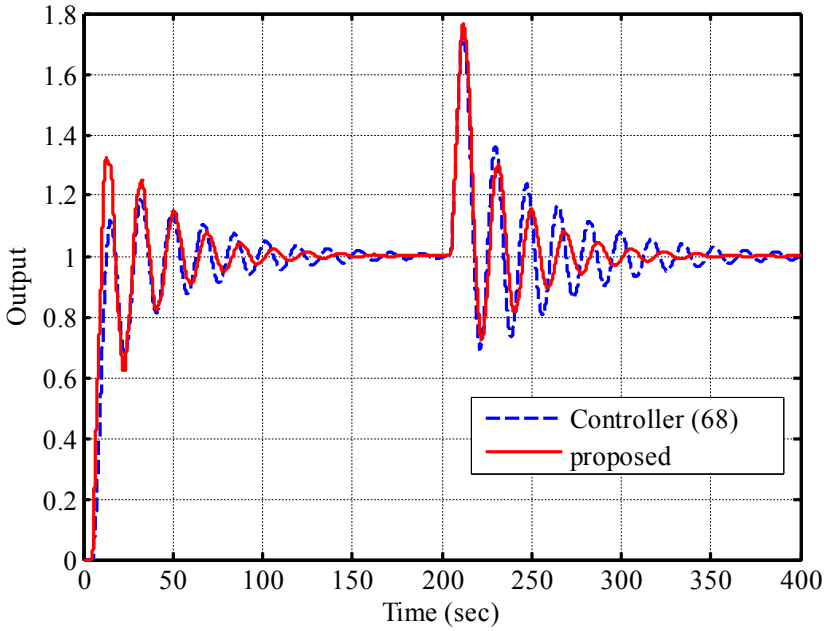


Figure 6: Time responses of Example 2 perturbed plant (+30%)

Table 1: Time characteristics for Example 2

	Set point			Disturbance		
	IAE	ISE	TV(u)	VIAE	ISE	TV(u)
nominal						
Method [42]	10.9061	8.1535	5.1347	**5.5827**	**1.7472**	0.6602
Proposed	**9.0633**	**6.2128**	**0.0119**	6.1389	2.0322	**0.0090**
15%						
Method [42]	10.9021	8.1395	3.5020	**5.6885**	**2.2235**	2.3133
Proposed	**9.1172**	**6.4505**	**0.0220**	6.1389	2.5236	**0.0153**
30%						
Method [42]	19.1074	9.4353	5.1495	18.7857	5.2353	3.1795
Proposed	**17.3068**	**8.4477**	**0.0724**	**13.7562**	**4.6458**	**0.0503**

6.3. Example 3

Consider the second-order integrative with time delay (SOIPDT) process presented in [36]:

$$P(s) = \frac{0.2}{s(1+4s)} e^{-s}. \tag{69}$$

This system was controlled in [36] using a Robust shifted-IMC controller given by:

$$\begin{aligned} G_{c1}(s) &= 0.039\left(1+\frac{1}{1.361s}\right), \\ G_{c2}(s) &= 0.195\,(1+1.933s)\,. \end{aligned} \tag{70}$$

This controller achieved a maximum sensitivity value of $M_s = 1.417$, indicating a moderate level of robustness against model uncertainties.

The proposed controller is given by:

$$\begin{aligned} G_{c1}(s) &= \frac{5\,(1+4s)\,0.6432^{1.1}}{s^{0.1}}, \\ G_{c2}(s) &= \frac{s\,(1+4s)\left(1+11.57s+30.28s^2\right)}{(1+3.52s)^3} \quad (M_s = 1.417)\,, \\ G_{c2}(s) &= \frac{s\,(1+4s)\,(1+6.93s+13.33s^2)}{(1+1.98s)^3} \quad (M_s = 1.8) \end{aligned} \tag{71}$$

the first controller ($M_s = 1.417$) is designed to enable a fair comparison with the Robust Shifted-IMC controller of [36]. The second controller ($M_s = 1.8$) demonstrates the flexibility of the proposed tuning approach, which allows achieving enhanced dynamic performance by exploiting the trade-off governed by the design parameter T_o.

Another PI-PD controller has been proposed for the same plant in [43].

$$\begin{aligned} G_{c1}(s) &= 1.49\left(1+\frac{1}{3.57s}\right), \\ G_{c2}(s) &= 2.45\left(1+\frac{3.51s}{1+0.351s}\right). \end{aligned} \tag{72}$$

The simulation was performed by applying a unit step change in the set-point at $t = 0$ sec, followed by a load disturbance applied at $t = 50$ sec. Figures 7, 8, and 9 illustrate the corresponding time responses for the nominal plant, the plant with +30% parameter variation, and the plant with +60% variation in both gain and time delay, respectively.

From these results, it can be observed that the proposed controller ensured satisfactory performance under all tested conditions. Specifically, the design with $M_s = 1.8$ exhibits faster transient behavior and improved disturbance rejection, while preserving adequate robustness up to +30% parameter variation. Conversely, the controller designed for $M_s = 1.417$ demonstrated slightly reduced nominal performance in but maintains robust behavior under severe uncertainty levels of up to +60%. These findings confirm the flexibility of the proposed tuning

approach in effectively balancing robustness and performance according to the selected M_s value.

Table 2 summarizes the all performance indices for all controllers under three operating conditions: nominal and perturbed cases with +30% and +60% varia-

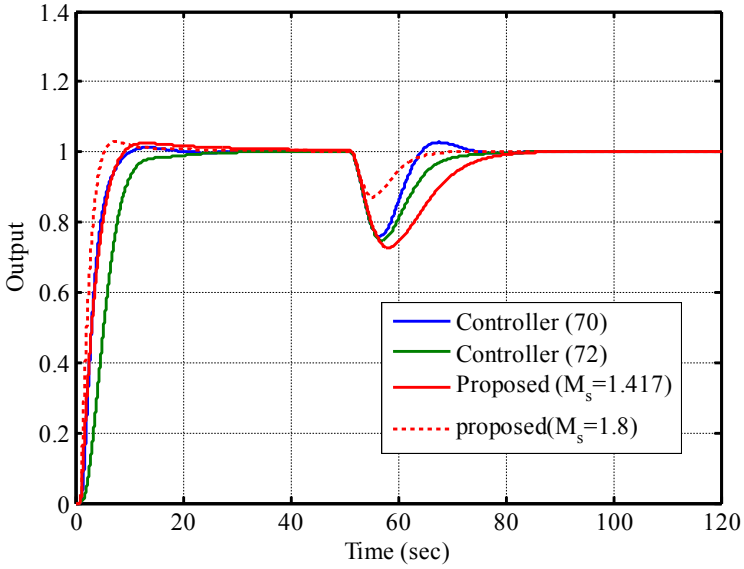


Figure 7: Time responses of Example 3 for nominal case

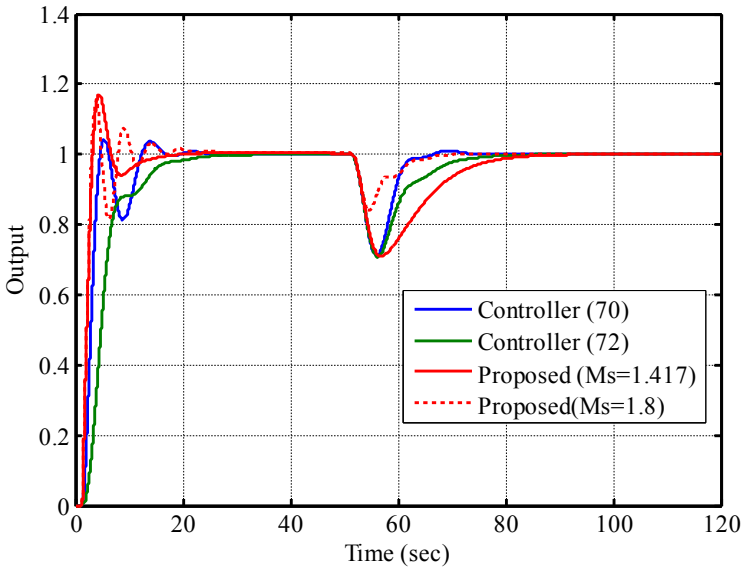


Figure 8: Time responses of Example 3 for perturbed case (+30%)

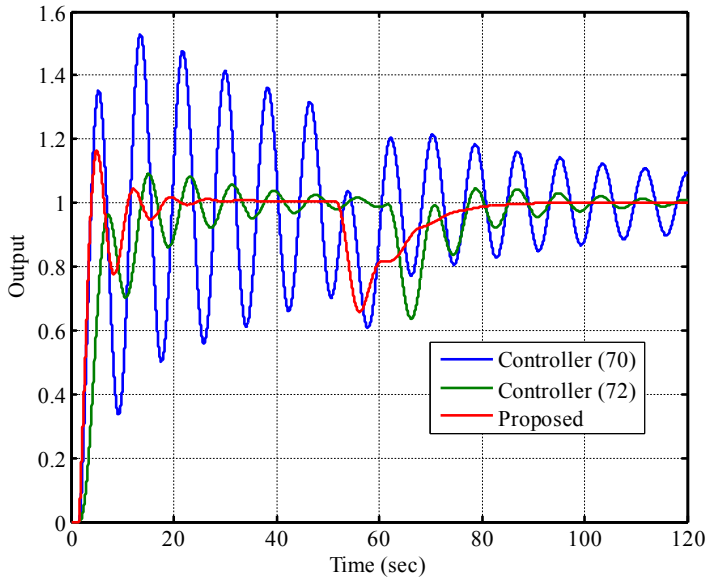


Figure 9: Time responses of Example 3 for perturbed case (+60%)

Table 2: Time characteristics for Example 3

	Set point			Disturbance		
	IAE	ISE	TV(u)	VIAE	ISE	TV(u)
nominal						
Method [36]	3.5798	2.5202	**1.1213**	1.8893	0.3094	0.4739
Method [43]	5.8749	4.2385	5.0508	2.3930	0.4115	2.7928
Prop. M_s = 1.42	4.1614	2.4434	3.5572	3.6832	0.6934	**0.2416**
Prop. M_s = 1.8	**2.8071**	**1.7999**	6.8577	**1.0410**	**0.0873**	0.4421
+30%						
Method [36]	3.7733	2.5469	4.3456	1.6408	0.3270	0.8891
Method [43]	5.8749	4.0399	4.0826	2.3930	0.4245	4.7749
Prop. M_s = 1.42	3.7688	2.3107	**3.8906**	3.6633	0.6926	**0.0672**
Prop. M_s = 1.8	**3.5641**	**1.9482**	10.4424	**1.1273**	**0.0911**	0.2432
+60%						
Method [36]	23.6705	8.4027	12.4710	6.9760	0.8285	7.2628
Method [43]	7.4885	4.2087	5.8361	**3.1970**	**0.5471**	4.6846
Prop. M_s = 1.42	**4.3754**	**2.5393**	**4.5112**	3.7153	0.7148	**0.1677**
Prop. M_s = 1.8	–	–	–	–	–	–

tions in process gain and delay. The results indicate that the proposed controller achieves better tracking performance under nominal conditions and maintains superior robustness under significant parameter perturbations.

Figure 10 illustrates the effect of white noise on the control input signal for the three considered controllers. The proposed controller, designed with $M_s = 1.41$, is included for comparison.

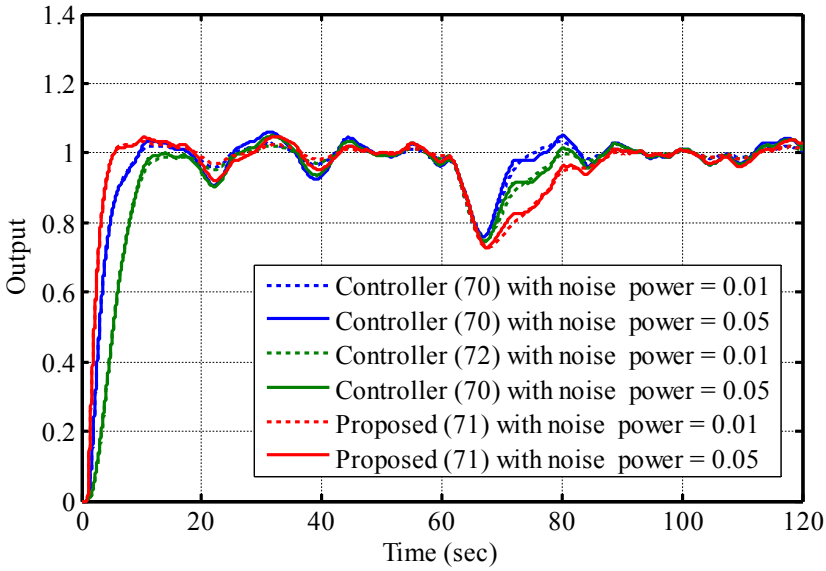


Figure 10: Time responses of Example 3 under noisy control input

6.4. Experimental validation

6.4.1. Description of the laboratory system

The experimental setup used in this study is a liquid level and flow control system (Fig. 11), representative of a class of the FOPTD process often found in industrial applications. The system is installed in the Control Laboratory of the

Table 3: Components of the Liquid Level Control System

1: LabJack U3-LV	2: Adaptation of the signals	3: USB cable	4: Laptop
5: Reservoir	6: Hand valve	7: On/Off valve	8: Pump
9: Pipe	10: Flow sensor	11: Proportional valve	12: Tank
13: Level sensor	14: Panel of the level & flow transmitters, supply and control		

Department consists of the following main components:

$$P(s) = \frac{0.608}{1 + 78s} e^{-25s}. \tag{73}$$

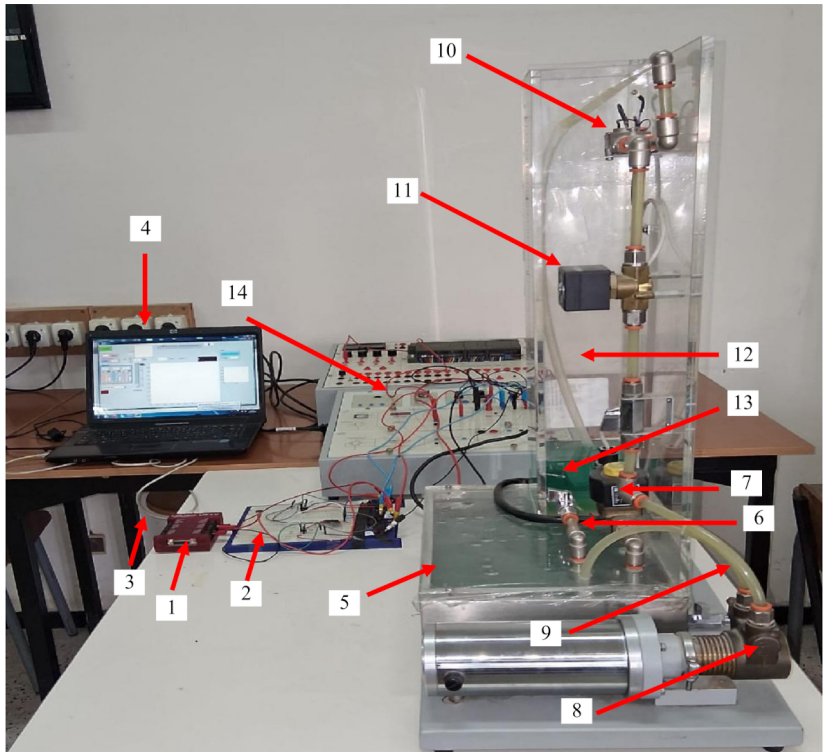


Figure 11: Experimental test bench components

6.4.2. Experimental results

To highlight the interaction between the two isolated loops in the proposed control structure, the following controller is implemented:

$$\begin{aligned} G_{c1}(s) &= \frac{1.65\,(1 + 78s)\,0.03^{1.1}}{s^{1.1}} \qquad M_s = 2.34, \\ G_{c2}(s) &= \frac{1.65\,(1 + 78s)\,(1 + 62.91s)}{(1 + 37.68s)^2} \qquad M_s = 1.5. \end{aligned} \tag{74}$$

The controller is designed to to provide higher robustness in the disturbance-rejection loop than in the reference-tracking loop. At ($t = 0$ sec), a reference step of magnitude 3 is applied, while an additive load disturbance of amplitude 2.87 is introduced at ($t = 300$ sec).

The experimental time responses of the plant controlled by (74) are shown in Figure 12. Two cases are considered: the nominal plant and the perturbed plant with (+20%) variation in both static gain and time delay. The results clearly demonstrate excellent tracking and disturbance-rejection performance for both nominal and perturbed conditions.

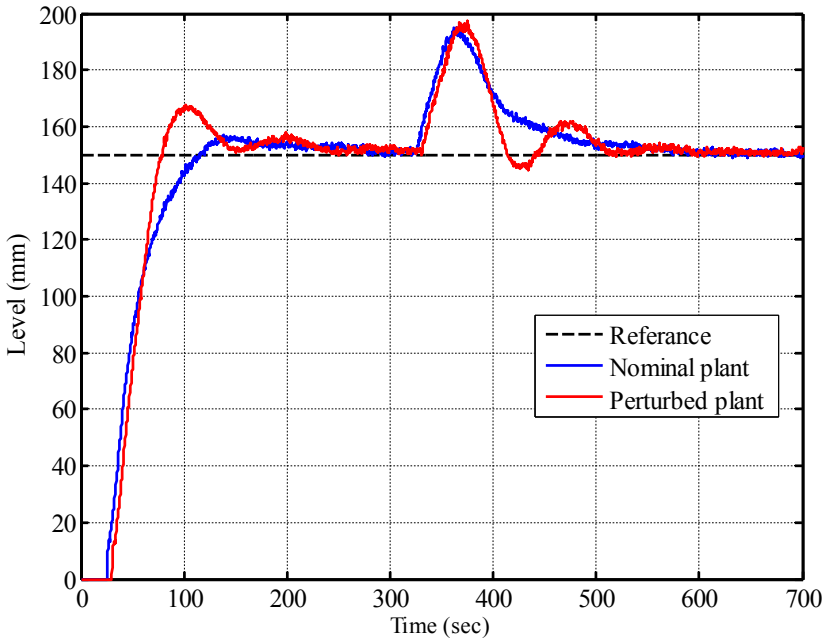


Figure 12: Time responses using controller (74)

Despite the high sensitivity associated with the tracking controller, the overall robustness of the proposed control scheme is preserved. Figure 13 presents the corresponding control efforts generated by the controllers for both cases.

To further illustrate the interaction between the two loops, the following controller is implemented:

$$\begin{aligned} G_{c1}(s) &= \frac{1.65\,(1+78s)\,0.055^{1.1}}{s^{1.1}} \qquad M_s = 1.8, \\ G_{c2}(s) &= \frac{1.65\,(1+78s)\,(1+44.54s)}{(1+17.95s)^2} \qquad M_s = 2. \end{aligned} \tag{75}$$

This controller is designed to provide higher robustness in the reference-tracking loop than in the disturbance-rejection loop. The experimental time responses and the corresponding control efforts are shown in Figs. 14 and 15, respectively.

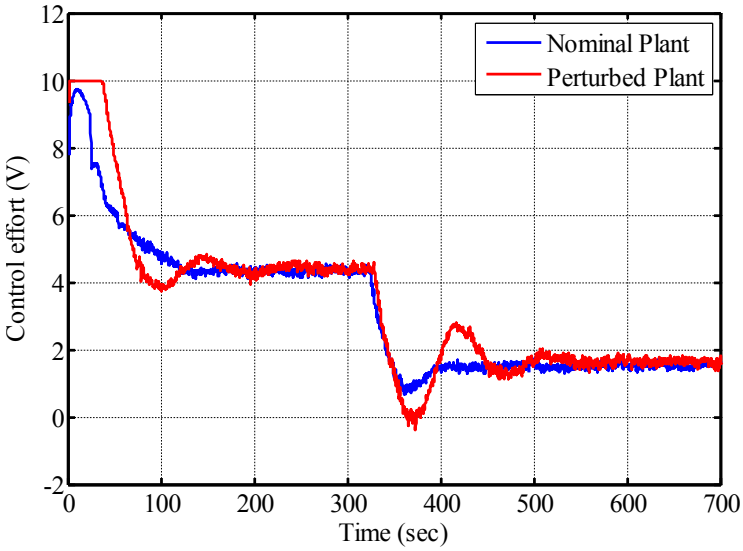


Figure 13: Control effort using controller (74)

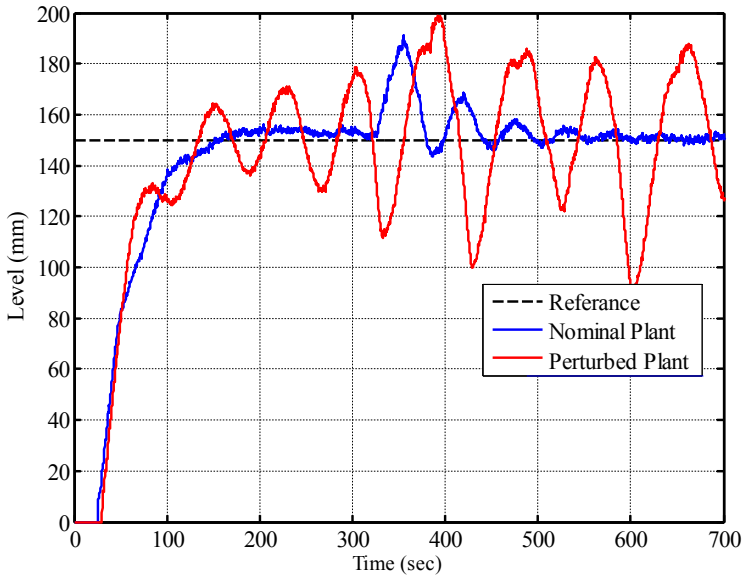


Figure 14: Time responses using controller (75)

The obtained results indicate that the disturbance-rejection loop plays a dominant role in determining the overall robustness of the plant with respect to parameter variations. Consequently, controller (75) exhibits lower robustness compared with controller (74).

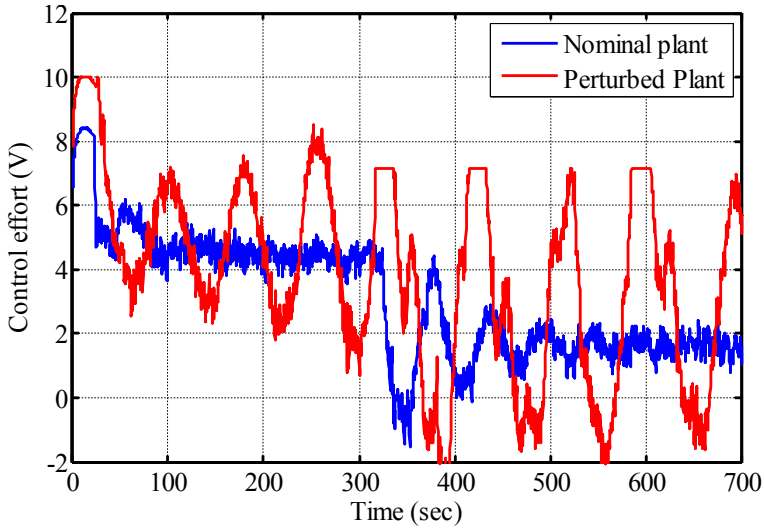


Figure 15: Control effort using controller (75)

The main advantage of employing a time-delay compensator becomes evident in systems with long time delays. For this reason, the time delay of system (73) is increased via software to obtain the following delay-dominated system:

$$P(s) = \frac{0.608}{1 + 78s} e^{-100s}. \tag{76}$$

The proposed controller is given by:

$$\begin{aligned} G_{c1}(s) &= \frac{1.65\,(1 + 78s)\,0.0103^{1.1}}{s^{1.1}} \qquad M_s = 4, \\ G_{c2}(s) &= \frac{1.65\,(1 + 78s)\,(1 + 77.97s)}{(1 + 75.74s)^2} \qquad M_s = 1.5. \end{aligned} \tag{77}$$

Times response and control effort of the plant (76) controller by (77) is shown in Figure 16 where the same disturbance is introduced at $t = 500$ sec. It is clearly observed that disturbance attenuation is significantly reduced as the time delay increases. This phenomenon is fundamentally related to the internal time delay: the effect of the load disturbance appears at the system output after θ seconds, and the corrective action of the controller requires an additional θ seconds. Consequently, a total duration of approximately 2θ seconds is needed to observe effective disturbance rejection.

Nevertheless, the reference-tracking performance remains satisfactory, and the disturbance is ultimately rejected, although with a larger impact on the output

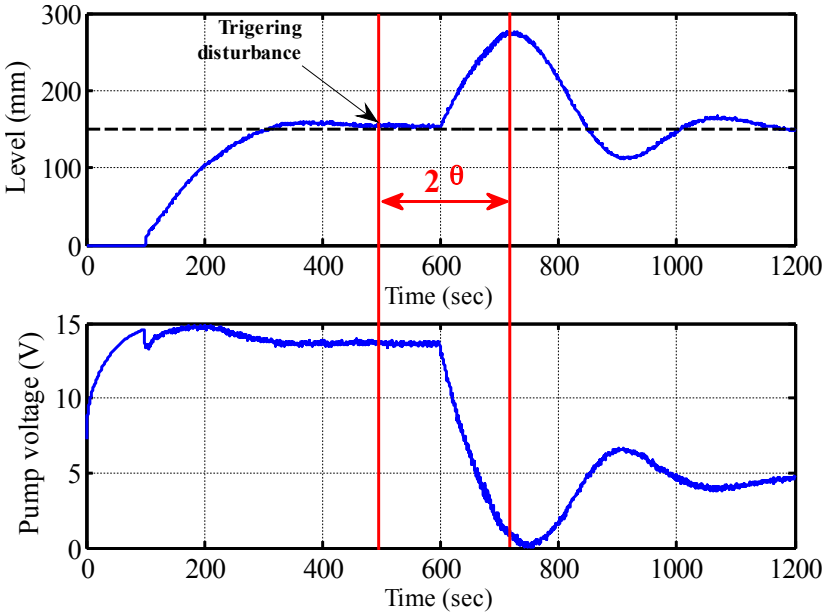


Figure 16: Nominal plant (76) controlled by (77)

compared to the case with a smaller time delay ($\theta = 25$ s). Moreover, the proposed controller generates a smooth control effort despite the increased delay.

7. Conclusions

An analytical robust controller has been developed for time-delay systems based on an isolated-loops Smith predictor structure. The proposed design approach employs Cardano's explicit solutions for cubic and quartic polynomial equations to derive optimal controller parameters that achieve a balanced trade-off between performance and robustness.

The effectiveness of the proposed method was first validated through extensive simulation studies involving various integrative process models, and comparisons with recent control strategies. The results demonstrate that the proposed controller achieves superior robustness compared to all other controllers designed for the same robustness metric (M_s), demonstrating the benefit of the isolated loop used structure.

Furthermore, the proposed control strategy was experimentally validated on a liquid level control system representative of FOPTD industrial processes. Experimental results under nominal and perturbed conditions confirm the simulation findings, demonstrating excellent reference-tracking performance, effective disturbance rejection, and smooth control effort generation, even in the presence

of significant time delays. In delay-dominated scenarios, the experimental analysis clearly illustrates the inherent limitation imposed by internal time delays on disturbance attenuation, while maintaining closed-loop stability and acceptable performance

The analysis of the two sensitivity functions confirms that the sensitivity associated with the disturbance-rejection loop has the dominant influence on robustness with respect to plant parameter variations. This feature provides the designer with practical flexibility to synthesize performance-oriented, robustness-enhanced, or intermediate controller configurations according to the desired design objectives.

CRediT authorship contribution statement

Nadir Fergani: Writing – review & editing, Writing – original draft, Software, Methodology, Investigation, Conceptualization. Mourad Allad: Validation, Investigation, Formal analysis, Ressources.

Disclosure statement

No potential conflict of interest was reported by the author(s).

References

[1] J.E. Normey-Rico and E.F. Camacho: *Control of dead-time processes*, Springer, London, 2007. DOI: 10.1007/978-1-84628-829-6

[2] O.J. Smith: A controller to overcome dead time, *ISA Journal*, **6**, (1959), 28–33.

[3] K.J. Astrom, C.C. Hang, and B. Lim: A new Smith predictor for controlling a process with an integrator and long dead-time. *IEEE Transactions on Automatic Control*, **39**, (1994), 343–345. DOI: 10.1109/9.272329

[4] C. Hang, Q.-G. Wang, and X.-P. Yang: A modified Smith predictor for a process with an integrator and long dead time. *Industrial & Engineering Chemistry Research*, **42**, (2003), 484–489. DOI: 10.1021/ie010881y

[5] K. Watanabe and M. Ito: A process-model control for linear systems with delay. *IEEE Transactions on Automatic Control*, **26**, (1981), 1261–1269. DOI: 10.1109/TAC.1981.1102802

[6] J.E. Normey-Rico and E.F. Camacho: Unified approach for robust dead-time compensator design. *Journal of Process Control*, **19**, (2009), 38–47. DOI: 10.1016/j.jprocont.2008.02.003

[7] S. Karan, C. Dey, and S. Mukherjee: Simple internal model control based modified Smith predictor for integrating time delayed processes with real-time verification. *ISA Transactions*, **121**, (2022), 240–257. DOI: 10.1016/j.isatra.2021.04.008

[8] S. Karan and C. Dey: IMC based modified Smith predictor for second order delay dominated processes with RHP. *ISA Transactions*, **142**, (2023), 254–269. DOI: 10.1016/j.isatra.2023.08.009

[9] S. Taherinasab, S. Soleimaniasl, and S. Taherinasab: Application of model reference adaptive control and modified Smith predictor to control blood glucose in type 1 diabetic patients. *Mathematics and Computers in Simulation*, **194**, (2022), 198–209. DOI: 10.1016/j.matcom.2021.05.033

[10] S. Kissoum, S. Ladaci, and A. Charef: Smith predictor PID-based robust adaptive gain-scheduled control for a class of fractional order LPV systems with time delays. *International Journal of Dynamics and Control*, **11**, (2023), 3096–3108. DOI: 10.1007/s40435-023-01175-9

[11] S. Tavakoli: A two-degree-of-freedom modified Smith predictor for teaching-friendly control of unstable systems with time delay. *International Journal of Dynamics and Control*, **12**, (2024), 4171–4177. DOI: 10.1007/s40435-024-01492-7

[12] S. Tavakoli: Analytical design of modified Smith predictor for second-order stable time delay plants incorporating a zero. *Franklin Open*, **8**, (2024), 100140. DOI: 10.1016/j.fraope.2024.100140

[13] R.D. Pereira, B.C. Torrico, J.N. Do Nascimento Jr, T.A. Lima, M.P. de Almeida Filho, and F.G. Nogueira: Smith predictor-based feedforward controller for measurable disturbances. *Control Engineering Practice*, **133**, (2023), 105439. DOI: 10.1016/j.conengprac.2023.105439

[14] B.C. Torrico, J.S. Barros, F.J. Vasconcelos, F.G. Nogueira, and J.E. Normey-Rico: Control of cascaded series dead-time processes with ideal achievable disturbance attenuation using a predictors-based structure. *Journal of Process Control*, **137**, (2024), 103193. DOI: 10.1016/j.jprocont.2024.103193

[15] Y. Wang, T. Huang, D. Yang, Z. Zhu, L. Cai, and K. Song: Dual-loop optimization of digital accelerometers based on advanced dual-degree-of-freedom Smith predictor. *ISA Transactions*, (2025). DOI: 10.1016/j.isatra.2025.07.009

[16] L. Liu, P. Du, Z. Sajid, B. Wilhite, C. Kravaris, and F. Khan: Experimental validation of the RESPONSE framework against cyberattacks on cyber-physical process systems. *AIChE Journal*, (2026), e70269. DOI: 10.1002/aic.70269

[17] V. Feliu-Batlle, R.R. Pérez, F.C. García, and L.S. Rodriguez: Smith predictor based robust fractional order control: Application to water distribution in a main irrigation canal pool. *Journal of Process Control*, **19**, (2009), 506–519. DOI: 10.1016/j.jprocont.2008.05.004

[18] D. Boudjehem, M. Sedraoui, and B. Boudjehem: A fractional model for robust fractional order Smith predictor. *Nonlinear Dynamics*, **73**, (2013), 1557–1563. DOI: 10.1007/s11071-013-0885-9

[19] T.N.L. Vu and M. Lee: Smith predictor based fractional-order PI control for time-delay processes. *Korean Journal of Chemical Engineering*, **31**, (2014), 1321–1329. DOI: 10.1007/s11814-014-0076-5

[20] M. Bettayeb, R. Mansouri, U. Al-Saggaf, and I.M. Mehedi: Smith predictor based fractional-order-filter PID controllers design for long time delay systems. *Asian Journal of Control*, **19**, (2017), 587–598. DOI: 10.1002/asjc.1385

[21] M. Safaei and S. Tavakoli: Smith predictor based fractional-order control design for time-delay integer-order systems. *International Journal of Dynamics and Control*, **6**, (2018), 179–187. DOI: 10.1007/s40435-017-0312-z

[22] S.H. Nagarsheth and S.N. Sharma: The combined effect of fractional filter and Smith Predictor for enhanced closed-loop performanceof integer order time-delay systems: some investigations. *Archives of Control Sciences*, **30**(1), (2020), pp. 47–76. DOI: 10.24425/acs.2020.132585

[23] Z. Shi and X. Yang: Analysis of Adaptive Fractional-Order Sliding-Mode Control Method Based on Smith Predictor for Voice Coil Motor. *Applied Sciences*, **16**(2), (2026), 620. DOI: 10.3390/app16020620

[24] S. Laifa, B. Boudjehem, and H. Gasmi: Direct synthesis approach to design fractional PID controller for SISO and MIMO systems based on Smith predictor structure applied for time-delay non integer-order models. *International Journal of Dynamics and Control*, **10**(3), (2022), 760–770. DOI: 10.1007/s40435-021-00831-2

[25] S.K. Vavilala and V. Thirumavalavan: Tuning of the two degrees of freedom FOIMC based on the Smith predictor. *International Journal of Dynamics and Control*, 9, (2021), 1303-1315. DOI: 10.1007/s40435-020-00742-8

[26] F.N. Deniz: An effective Smith predictor based fractional-order PID controller design methodology for preservation of design optimality and robust control performance in practice. *International Journal of Systems Science*, **53**(14), (2022), 2948–2966. DOI: 10.1080/00207721.2022.2067366

[27] G. Saikumar, K.K. Sahu, and P. Saha: Design of fractional-order IMC for nonlinear chemical processes with time delay. *International Journal of Dynamics and Control*, **11**(4), (2023), 1797–1807. DOI: 10.1007/s40435-022-01087-0

[28] A. Ranjan, U. Mehta, S. Prakash, and S.I. Azid: Direct synthesis approach to design PD$^{\mu}$ based smith predictor for integrating plants: Studied on a quadrotor UAV. *The Journal of Engineering*, **2024**(4), (2024), e12378. DOI: 10.1049/tje2.12378

[29] S. Karan and C. Dey: A review on modified Smith predictor schemes for delay dominated processes. *Chemical Product and Process Modeling*, (2026). DOI: 10.1515/cppm-2025-0160

[30] A. Ranjan and U. Mehta: Fractional-order tilt integral derivative controller design using IMC scheme for unstable time-delay processes. *Journal of Control, Automation and Electrical Systems*, **34**, (2023), 907–925. DOI: 10.1007/s40313-023-01020-6

[31] C.I. Muresan and I. Birs: Fractional order control for unstable first order processes with time delays. *Fractional Calculus and Applied Analysis*, **27**, (2024), 1709–1733. DOI: 10.1007/s13540-024-00301-4

[32] S.H. Nguyen, V.N. Truong, and L.N. Nguyen: Analytical tuning rules for cascade control systems based on fractional-order PI controller in frequency domain. *IEEE Access*, **11**, (2023), 76196–76201. DOI: 10.1109/ACCESS.2023.3296496

[33] P. Singha, R. Meena, and S. Chakraborty: 2-DOF fractional-order control for delay-dominant industrial processes with experimental validation. *International Journal of Dynamics and Control*, **13**(2), (2025), 72. DOI: 10.1007/s40435-024-01574-6

[34] P. Singha, R. Meena, S. Chakraborty, and G.L. Raja: Robust pidf-pid cascade control scheme for delay-dominant stable and integrating chemical processes. *Journal of the Taiwan Institute of Chemical Engineers*, **173**, (2025), 106165. DOI: 10.1016/j.jtice.2025.106165

[35] R. Meena, S. Chakraborty, and V. Chandra Pal: Designing a dual parametric fractional controller for delayed stable/unstable/integrating processes with experimental validation. *International Journal of Systems Science*, **57**(3), (2026), 759–776. DOI: 10.1080/00207721.2025.2511213

[36] P. Aryan, V. Kumar, G.L. Raja, T.R. Chelliah, and Y. V. Hote: Robust shifted-IMC based modified decoupled Smith predictor for delay-dominant integrating-type chemical processes. *International Journal of Systems Science*, **57**(3), (2026), 740–758. DOI: 10.1080/00207721.2025.2510313

[37] P. Singha, D. Das, R. Meena, and S. Chakraborty: Experimentally validated predictive dual parametric fractional-order tuning approaches for time delayed chemical processes. *Journal of the Taiwan Institute of Chemical Engineers*, **180**, (2026), 106463. DOI: 10.1016/j.jtice.2025.106463

[38] P. Singha, D. Das, and S. Chakraborty: Predictive tuning strategies for different classes of delay dominant chemical processes. *Journal of the Taiwan Institute of Chemical Engineers*, **181**, (2026), p. 106570. DOI: 10.1016/j.jtice.2025.106570

[39] A. Oustaloup: *La commande CRONE: commande robuste d'ordre non entier*. Paris: Hermes, 1991.

[40] N. Fergani, N. Boutasseta, and I. Attoui: An explicit tuning of the fractional order controller using a novel time delay approximation. *International Journal of Dynamics and Control*, **11**, (2023), 2410–2422. DOI: 10.1007/s40435-023-01132-6

[41] S. Karan and C. Dey: Modified Smith predictor-based all-proportional-derivative control for second-order delay-dominated integrating processes. *Asia-Pacific Journal of Chemical Engineering*, **16**(2), (2021), e2591. DOI: 10.1002/apj.2591

[42] P. Singha, D. Das, S. Chakraborty, and G.L. Raja: Experimentally validated predictive PI-PD control strategy for delay-dominant chemical processes. *Chemical Engineering Science*, **295**, (2024), 120197. DOI: 10.1016/j.ces.2024.120197

[43] M. Irshad and A. Ali: Robust PI-PD controller design for integrating and unstable processes, *IFAC-PapersOnLine*, **53**(2), (2020), 135–140. DOI: 10.1016/j.ifacol.2020.06.023